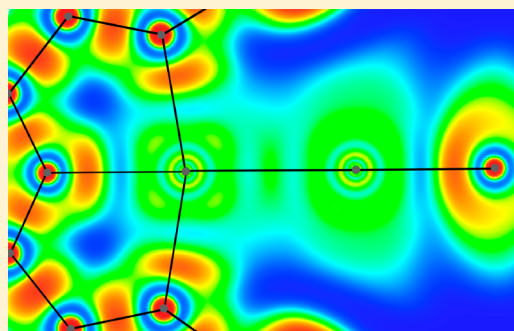


Influence of Relativistic Effects on Bonding Modes in M(II) Dinuclear Complexes (M = Au, Ag, and Cu)

Paul Jerabek,^{*,†} Beatriz von der Esch,[†] Hubert Schmidbauer,^{*,‡} and Peter Schwerdtfeger^{*,†}[†]The New Zealand Institute for Advanced Study, Massey University, Private Bag 102904, 0632 Auckland, New Zealand[‡]Department Chemie, Technische Universität München, 85747 Garching, Germany

Supporting Information

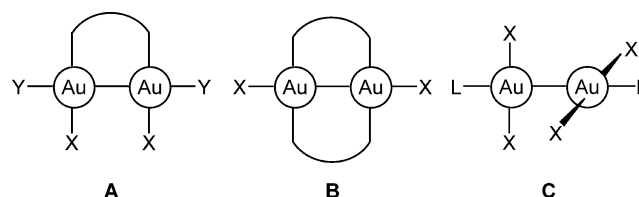
ABSTRACT: The stability and bonding in dinuclear group 11 metal complexes (M = Au, Ag, and Cu) in their +2 oxidation state has been investigated by quantum chemical methods. Two model complexes were selected as representatives of different bonding situations in the dinuclear M(II) complexes, a direct metal–metal bond between two ligand stabilized monomers and ligand-mediated bridged dimer system, making them interesting for a direct comparison and to study the influence of relativistic effects. Relativity substantially stabilizes the direct metal–metal bonded system obtaining the sequence in M–M bond stability Au > Ag > Cu. In the ligand-bridged structure, an asymmetric bonding situation is obtained for gold, resulting in two stronger/covalent and two weaker/ionic bonds per gold atom. Here we observe the opposite trend in stability Cu > Ag > Au. Our analysis nicely corroborates with what is known from experimental observation.



INTRODUCTION

The composition, structure and bonding characteristics of complexes of the coinage metals Au, Ag, and Cu in their +2 oxidation state with an nd^9 ($n = 3, 4,$ and 5) electronic configuration is surprisingly diverse. For gold, the Au^+ and Au^{3+} states (with the electronic configurations $5d^{10}$ and $5d^8$, respectively) are the most common oxidation states, and complexes of Au^{2+} (with $5d^9$) are extremely rare.¹ This is particularly true for mononuclear complexes, which are known only for species with a ligand or a set of ligands providing a rigid and redox-stable environment for the metal center, e.g., as in phthalocyanines and porphyrins.² These complexes are paramagnetic and show a magnetic moment corresponding to the spin-only value for the unpaired electron in $5d^9$ ($\mu_{\text{eff}} = 1.79 \mu_B$) and typically an ESR quartet signal (the nuclear spin of ^{197}Au is $I = 3/2$). Dinuclear complexes of Au^{2+} are also small in number, but they are found to be exclusively diamagnetic owing to structures with close Au–Au contacts of about 2.6 Å, which appear to represent true covalent Au–Au σ -bonding.³ This situation arises predominantly in “ligand-supported” frames, where one or two 1,3- or 1,4-difunctional donors bridge the two Au^{2+} centers present as a Au_2^{4+} core unit (A, B) as shown in Scheme 1.⁴ However, very recently, a few cases with “ligand-unsupported” $Au^{\text{II}}-Au^{\text{II}}$ bonding have also been reported where the same short Au–Au distances are found as the only connectivity between the mononuclear units (C), see also Scheme 2.⁵ The issue of ligand supported vs unsupported dinuclear complexes has recently been addressed by Xiong and Pyykkö.³

For silver, the Ag^+ state by far dominates the chemistry of this element. This is true not only for silver minerals but also

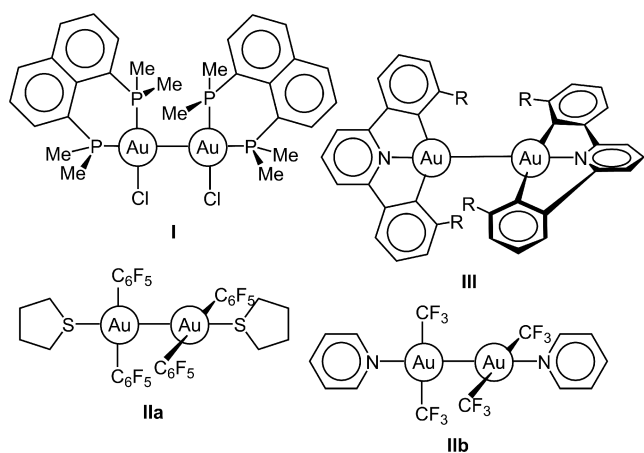
Scheme 1. Illustration of Different $Au^{\text{II}}-Au^{\text{II}}$ Bonding Modes

for the aqueous system regardless of the presence of air or an inert atmosphere. The Ag^{3+} state has been shown to be accessible only with the strongest oxidants, and Ag^{2+} is found almost exclusively with redox-robust ligands with fluorine or oxygen donor atoms.⁶ A most interesting pair of examples has been provided with the black, paramagnetic, and unstable $Ag^{\text{II}}\text{SO}_4$ and its colorless, diamagnetic, and stable “isomer” $(Ag^{\text{I}})_2(\text{S}_2\text{O}_8)$.^{6,7} However, it is most intriguing that diamagnetic di- or polynuclear Ag^{2+} complexes are completely absent in the literature, except for some reactive compounds in the gas phase.⁸ No crystal structures of silver(II) compounds have been reported which would indicate discrete $Ag^{\text{II}}-Ag^{\text{II}}$ bonding. There are cases of magnetic ordering in crystals of silver(II) compounds at low temperature, but diamagnetism is not reached in any of the known examples. Instead, $Ag^{\text{II}}\text{SO}_4$ is antiferromagnetic indicating significant spin transfer to the ligand environment, with both effects being much stronger than those in anhydrous $Cu^{\text{II}}\text{SO}_4$.

Received: September 26, 2017

Published: November 14, 2017

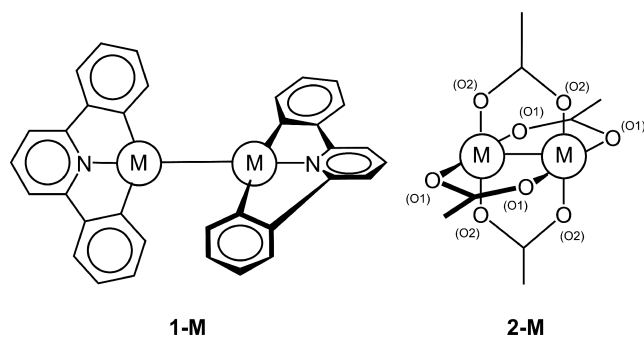
Scheme 2. Dimers with Ligand-Unsupported Au^{II}–Au^{II} Bonding



Finally, for copper, it is the Cu²⁺ state which accounts for the majority of the minerals and of the salts and complexes appearing in aqueous systems under standard conditions, while Cu⁺ is produced only under reducing conditions with what is known as “soft ligands”. By contrast, with “hard ligands”, as in the aqueous environment, Cu⁺ is subject to disproportionation to give copper metal, Cu⁰, and more strongly solvated Cu²⁺. In this context, it is worth remembering that Ag⁺ has never been shown to disproportionate in water into Ag⁰ and Ag²⁺ while Au⁺ disproportionates in water to give Au⁰ and Au³⁺. These discrepancies have all been rationalized by measurements and calculations of the redox potentials of the species involved with a broad spectrum of ligands and in a variety of solvents.⁹ One of the unexplained phenomena in copper(II) chemistry, as in silver(II) chemistry, is the complete absence of Cu^{II}–Cu^{II} bonding that would be characterized by diamagnetism and by the absence of an ESR signal, as well as by a short Cu–Cu distance in any dinuclear complex. In numerous review articles, copper(II) complexes with a large variety of terminal, bridging, or chelating ligands with hard or soft donor atoms have been compiled, for which the structures have been determined and the magnetochemistry has been investigated, but there is no case with a diamagnetic dinuclear Cu₂⁴⁺ core unit, be it ligand-supported or not.¹⁰

In the light of these observations, in the present study the bonding in M^{II}–M^{II} units with M = Au, Ag, and Cu in different environments has been (re)investigated by quantum-chemical calculations on two model systems (Scheme 3). One type of

Scheme 3. Structures of Model Systems Calculated in This Work



compound (**1-M**) has been chosen based on one case out of the very few known species with ligand-unsupported Au^{II}–Au^{II} interactions.⁵ According to the experimental work on the parent gold compound (with four bulky *t*-butyl substituents, **I**),^{5e,f} all criteria of true σ -bonding are met (diamagnetism, ESR silence, short Au–Au distance of ~ 2.6 Å, large HOMO–LUMO gap, and free rotation about the Au–Au axis). The Au^{II}–Au^{II} bond enthalpy has been determined by electrochemical studies. The result (-198 ± 1 kJ/mol) is in agreement with calculations by Xiong and Pyykkö carried out for another example (**IIa**)⁵ of the four known ligand-unsupported cases (**I**, **IIa,b**, and **III**). There is no comparable case in silver and copper chemistry, as summarized above. For ligand-supported Au(II)–Au(II) units, the oxidation state of the metal atoms has been confirmed by ESCA and ¹⁹⁷Au Mössbauer spectra. The results rule out any mixed-valence alternative.¹¹

As a ligand-supported example of M^{II}–M^{II} interactions, framework **2-M** has been chosen which is found in dinuclear copper(II) acetate and its dihydrate (**2-Cu**).¹² This ligand-bridged dinuclear complex is one of the most extensively studied compounds in copper chemistry, mainly owing to its intriguing magnetochemical properties. The crystal structures of **2-Cu** and its dihydrate have been determined more than a dozen times including X-ray and neutron diffraction studies.^{12,13} For decades, researchers have tried to elucidate the contributions and the interplay of both direct Cu^{II}–Cu^{II} bonding (an antiferromagnetic interaction) and the ligand-mediated Cu(3d⁹)–Cu(3d⁹) interactions (which are ferromagnetic), which lead to the observed temperature-dependent magnetic properties.¹⁴ The system has once been considered “the archetypical weakly metal–metal interacting dimer”. In one of the most recent DFT studies, both Cu₂(OAc)₄·2H₂O and anhydrous Cu₂(OAc)₄ were again investigated with broken symmetry calculations arriving in an atoms-in-molecule model showing significant bond critical points for the Cu–Cu unit.^{13a} The results of these and related studies on **2-Cu** are discussed again below. However, no such studies have been performed with **2-Ag** or **2-Au**. There is no silver(II) acetate known in the literature because most carboxylate anions are readily oxidized by Ag²⁺.

The combination of gold(II) solely with acetate in the absence of auxiliary ligands leads to disproportionation into Au⁰ and Au³⁺. However, with powerful bridging ligands, like phosphorus ylides, stable gold(II) complexes with terminal acetate groups at the (Au^{II}–Au^{II}) core have been achieved.¹⁵ It is expected that the strongest of the M^{II}–M^{II} interactions will arise in the model **2-Au** even though the tendency toward disproportionation makes these systems intrinsically unstable. Moreover, the known preference of gold cations for low coordination numbers (CN = 2 for Au⁺, CN = 4 for Au³⁺) suggests a similar preference for Au²⁺. In the known complexes with the dinuclear Au₂⁴⁺ core unit, the gold atoms are all in a square planar environment, but the geometry is often codetermined by the chelating or bridging ligands. It is only in examples **IIa** and **IIb** that no such constraints apply, and therein the two C–Au bonds are unusually short compared to reference compounds, while the S–Au distances in **IIa** are relatively long, indicating the tendency to establish two particularly strong bonds in tetra-coordinate Au²⁺ complexes.^{5c} For model **2-Au**, unsymmetrical bridging by acetate may be anticipated reflecting this preference for two-coordination. No

such asymmetry has been observed for **2-Cu** complexes, and examples for **2-Ag** are not available.

This brief literature survey would be incomplete without mentioning the experimentally “nonexistent” AuO for which several structural variations have recently been calculated (under standard and elevated pressure). At ambient temperature, a mixed-valent structure is predicted where two-coordinate Au⁺ centers are featuring aurophilic interactions, while square-planar tetra-coordinated Au³⁺ centers are bridging elements. At higher pressure, a structure with Au₂⁴⁺ appears to be preferred with strong Au^{II}–Au^{II} bonding, but under extreme pressure a simple AB structure (NaCl, CsCl) may arise.¹⁶ By contrast, in CuO, the Cu²⁺ cations are in a standard square planar environment of O²⁻ anions with long distances between metal atoms,¹⁷ while the AgO polymorphs are again mixed-valent oxides with linearly two-coordinate Ag⁺ and square-planar coordinated Ag³⁺.¹⁸

It has been recognized in recent years that much of the diversity in coinage metal coordination chemistry originates from the increasing importance of relativistic effects in the triad Cu–Ag–Au.¹⁹ This applies to the increase in electronegativity, the extreme electrochemical potential for Au, the anomalies in the atomic/ionic radii of Ag and Au, the high 6s-character of gold orbitals involved in bonding, the decrease in coordination numbers, the stability of high oxidation states, and many other phenomena including the color of the metal.²⁰ Here we mention that relativistic effects in atomic and molecular properties usually scale like $\sim(Z\alpha)^2$ (Z being the nuclear charge and $\alpha \approx 1/137$ the fine structure constant), but with an unusually large prefactor for the group 11 (and 12) series of elements compared to the other groups in the periodic table.²¹ This originates from the filling of the lower lying polarizable d-orbitals screening the nucleus less effectively.²²

In contrast to dispersive type d¹⁰–d¹⁰ interaction for the group 11 metals,²³ theoretical studies on d⁹–d⁹ interactions are rare.^{3,24} The systematic study presented here will give direct evidence for the prime significance of relativistic effects in determining the surprisingly different characteristics of structure and bonding of homologous Cu/Ag/Au compounds in the oxidation state +2.

COMPUTATIONAL DETAILS

We selected the two model complexes, **1-M** and **2-M** ($M = \text{Cu, Ag, and Au}$), as representatives of the different bonding situations in the M(II) dimer complexes. **1-M** is used as an example for a direct metal–metal bond, while the bonding interactions in **2-M** are assumed to be mainly ligand-mediated, thus making them interesting for a direct comparison and to study the influence of relativistic effects. We used Orca 3.0.3 program package to optimize the various structures of **1-M** and **2-M**. For this, we tested several commonly used density functionals. From a comparison of bond lengths between the crystal structure of [(C[^]N[^]C)₂Au₂] (the symbol [^] indicates the bridge) and the optimized geometry of **1-Au**, we identified the hybrid functional B3LYP with Grimme’s D3 dispersion correction using the Becke–Johnson (BJ) damping function (D3-BJ)²⁵ as the best suited functional. The def2-TZVPP basis set was used²⁶ (abbreviated as B3LYP(D3-BJ)/def2-TZVPP or simply B3LYP for the following) utilizing the resolution of identity (RI) approximation.²⁷ For the coinage metal atoms, we applied the relativistic (R) and nonrelativistic (NR) energy-consistent Stuttgart effective core potentials (ECPs)^{20a,28} with the accompanying triple- ζ valence basis sets. From the Hessian, we ensured that the optimized structures are minima on the potential energy surface. The calculated bond dissociation energies ΔE were corrected by zero-point vibrational energies and thermodynamic contributions to the enthalpy ΔH ($T = 298.15 \text{ K}$, $P = 101 \text{ kPa}$). In

addition, quantum theory of atoms in molecules (QTAIM)²⁹ analyses were performed with the program Multiwfn.³⁰ Löwdin population analyses³¹ were obtained from these optimized structures, but with a def2-SVP all-electron basis set at nonrelativistic and relativistic level of theory, using the zero-order regular approximation (ZORA) for the latter.³² The electron localization functions (ELFs)³³ were calculated at the same level of theory.³⁰ For the singlet states of compounds **2-M**, the triplet ground state of the system is computed first and used as an initial guess for the broken symmetry singlet state in an unrestricted DFT Kohn–Sham procedure according to Noodleman’s broken symmetry approach (BS).²² This results in a single reference wave function with an energy lower than that of the triplet state in our case and that can also be used for estimating the antiferromagnetic coupling between the two metal centers.

RESULTS AND DISCUSSION

Direct Metal–Metal Bond (1-M). For the gold compound in **1-M**, our calculated B3LYP(D3-BJ)/def2-TZVPP bond lengths are slightly larger compared to the experimental results, i.e., compare the experimental bond distances $d(\text{Au–Au}) = 2.494 \text{ \AA}$, $d(\text{N–Au}) = 2.018 \text{ \AA}$, and $d(\text{C–Au}) = 2.084 \text{ \AA}$ with those in Table 1. In comparison to the nonrelativistic

Table 1. Selected Bond Lengths (Å) from Optimized Structures of **1-M** and **2-M** with (R) and without (NR) Inclusion of Relativistic Effects Calculated at the B3LYP(D3-BJ)/def2-TZVPP Level of Theory

	R			NR		
	M–M	M–N	M–C	M–M	M–N	M–C
1-Au	2.536	2.070	2.085	2.666	2.157	2.190
1-Ag	2.513	2.072	2.105	2.561	2.106	2.149
1-Cu	2.204	1.924	1.972	2.210	1.936	1.991
	M–M	M–O1	M–O2	M–M	M–O1	M–O2
2-Au	2.735	2.075	2.333	2.832	2.245	2.307
2-Ag	2.683	2.141	2.186	2.729	2.176	2.221
2-Cu	2.490	1.967	1.974	2.505	1.979	1.985

calculations, we see that the metal–metal optimized bond distances in **1-M** are substantially influenced by relativistic effects; compared to the nonrelativistic results, the M–M distances shorten by $\Delta_{\text{R}}d = 0.130 \text{ \AA}$ for Au, 0.048 \AA for Ag, and 0.006 \AA for Cu, respectively, due to relativity. This gives approximately $\Delta_{\text{R}}d[\text{\AA}] = 0.39(Z\alpha)^2$ for the group 11 elements. We note that in aurophilic interactions which are of dispersive type and dominated by electron correlation rather small relativistic effects have been found in the metal–metal bond lengths in the (XMPH₃)₂ compounds even for gold.²³

Concerning the metal–ligand interactions, it may be useful to compare the relativistic bond contractions with those obtained typically from Au(I) or Au(III) coordination compounds. For the AuX₂[−] complexes, one typically obtains $\Delta_{\text{R}}d = 0.18\text{--}0.20 \text{ \AA}$ depending on the ligand X ($X = \text{F, Cl, Br, and I}$), while for the AuX₄[−] complexes one has a far lesser effect, $\Delta_{\text{R}}d = 0.07\text{--}0.10 \text{ \AA}$. The reason for the diminished relativistic bond contractions when moving to higher oxidation state is well understood and is connected to the occupancy of the Au(6s) orbital. Here for the Au(II)–ligand relativistic bond contraction, we get rather small values, i.e., $\Delta_{\text{R}}d(\text{Au–N}) = 0.087 \text{ \AA}$ and $\Delta_{\text{R}}d(\text{Au–C}) = 0.105 \text{ \AA}$, in line with the higher oxidation state.

Table 2 shows Löwdin population analyses for the various compounds studied here. We clearly see that relativistic effects increase the valence n s population, and increase both the ($n -$

Table 2. Löwdin Atomic Charges q and Orbital Populations (e) for the Valence Shells of 1-M and 2-M with (R) and without (NR) the Inclusion of Relativistic Effects

M	R				NR			
	q	s	p	d	q	s	p	d
1-Au	-0.31	0.39	0.83	9.44	-0.25	0.24	0.75	9.63
1-Ag	0.69	0.25	0.60	9.30	0.62	0.21	0.58	9.38
1-Cu	0.29	0.21	0.90	9.92	0.29	0.20	0.89	9.95
2-Au	0.06	0.34	0.64	9.79	0.17	0.17	0.54	10.00
2-Ag	0.89	0.18	0.45	9.48	0.87	0.14	0.43	9.55
2-Cu	0.68	0.22	0.70	9.40	0.69	0.12	0.69	9.42

1)d and np orbital participations in the bonding, very similar to the results obtained previously for Au(I) and Au(III) coordination compounds.²⁰ The relativistic increase in the valence ns population down the group 11 elements correlates nicely with the relativistic bond contractions observed.

Typically, shorter bond lengths can be interpreted as stronger chemical bonding, and we therefore expect that relativistic effects lead to a bond strengthening in these Au–Au interactions. To quantify the influence of relativistic effects on the stability of the complexes, the bond dissociation energies ΔE (BDE) into the respective monomers were calculated, see Table 3 (the corresponding enthalpies ΔH can be found in

Table 3. Bond Dissociation Energies ΔE (in kJ/mol) of 1-M and 2-M into the Respective Monomers Calculated at B3LYP(D3)/def2-TZVPP Level of Theory with and without Relativistic Effects Included for the Metal Atoms^a

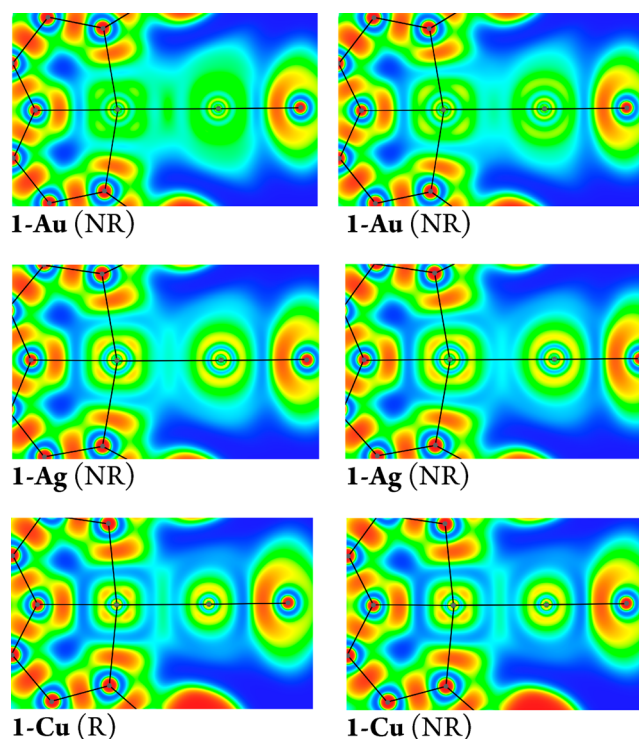
	relativistic			nonrelativistic		
	Au	Ag	Cu	Au	Ag	Cu
1-M S	286.0	201.2	188.5	184.5	160.2	181.7
	<i>101.5</i>	<i>41.0</i>	<i>6.8</i>			
2-M T	73.7	103.9	163.7	94.9	106.0	162.9
	<i>-21.2</i>	<i>-2.1</i>	<i>0.8</i>			
2-M S(BS)	91.3	110.8	166.9	111.5	111.2	166.6
	<i>-20.0</i>	<i>-0.4</i>	<i>0.3</i>			

^aFor 2-M both electronic configurations, the triplet (T) ground state and the broken-symmetry singlet (S(BS)), were calculated. Relativistic effects are shown in italics.

Table S1). Comparing the relativistic BDEs, the M–M bond stabilities follow the trend **1-Au > 1-Ag > 1-Cu**. The stability of the Ag–Ag interaction is 60 kJ/mol, and that of Cu–Cu interaction is 100 kJ/mol smaller compared to that of the corresponding gold dimer. Model complex **1-Au** is by far the most stable system and agrees with experimental observations as its parent compound has been isolated and characterized,^{5e,f} while there has not been any successful syntheses reported so far for the corresponding $[(C^{\wedge}N^{\wedge}C)_2Ag_2]$ or $[(C^{\wedge}N^{\wedge}C)_2Cu_2]$ species.

The situation changes drastically when the calculations are performed without relativistic effects included: The BDE for heavier coinage metal complexes **1-Au** and **1-Ag** become smaller by roughly 100 and 40 kJ/mol, respectively, while the effect for **1-Cu** is minor as expected (Table 3). This results in a different trend for the metal–metal bond stabilities **1-Au \approx 1-Cu > 1-Ag**. In other words, without relativistic effects, the metal–metal bond in the gold dimer would be as weak as that in the copper homologue. In fact, as with the bond distances, we get the scaling behavior for the bond dissociation energy ΔE with increasing nuclear charge as $\Delta_R \Delta E [kJ/mol] = 2.25(Z\alpha)^2$.

To get more insight into how relativistic effects influence the metal–metal bond for these complexes, we produced 2D plots of the corresponding electron localization function, Figure 1. It

**Figure 1.** ELF plots for the 1-M compounds at the relativistic (R) and nonrelativistic (NR) level of theory.

is clearly visible how localized electron density is concentrated in between the gold atoms of **1-Au** when comparing nonrelativistic with relativistic ELF plots. This is not the case for the copper species and to a much lesser extent for the silver compound. The reason for this lies in the high relativistically increased electronegativity of gold (2.4) compared to the much smaller value for copper and silver (1.9); note the negative atomic partial charge on Au in Table 2. This implies that both gold atoms withdraw electron density from the surrounding ligands and utilize this in establishing a stronger intermetallic bond.

Another noticeable feature is that for copper and silver the d-electron shell structure around the atoms is easily recognizable with high ELF values while the 5d-electrons of gold are more delocalized with less pronounced high ELF values. This is also reflected by the atomic Löwdin population analyses of the metal atoms (Table 2). In the relativistic case, the 6s orbital population is nearly twice as large ($\approx 0.4 e$) compared to the

nonrelativistic result ($\approx 0.2 e$). The 5d orbitals, in contrast, experience a loss of roughly $0.2 e$ when including relativistic effects. For silver, this change in valence orbital population is less pronounced, while it is negligible in the copper compound. The higher s and p orbital and lower d orbital occupations enhanced by relativistic effects are favorable for direct metal–metal bonding as they lead to stronger covalent interactions between the two metal atoms.

Ligand-Mediated Bonding (2-M). It is well-established that $[\text{Cu}_2(\text{OAc})_4 \cdot 2\text{H}_2\text{O}]$ possesses a singlet electronic state because of antiferromagnetic coupling between the unpaired electrons of the copper atoms. To a reasonable approximation, this can be modeled with Noodleman's broken symmetry (BS) approach as done here. (In principle, however, a multireference treatment is required.)^{13a,34}

The optimized structure (Table 1) for 2-Cu gives a shorter Cu–Cu bond length compared to the crystal structure value for $[\text{Cu}_2(\text{OAc})_4 \cdot 2\text{H}_2\text{O}]$ ($d(\text{Cu}–\text{Cu})$: 2.617 Å),¹² which to our opinion can be attributed mostly to the missing water molecules in our calculation. The other bond lengths are in rather good agreement with experiment. Note that the Au–O bonds are strongly asymmetrical in relativistic 2-Au, indicating that half of the oxygen atoms are more strongly bound to the gold atoms than the others while the M–O bonds are very similar in the copper and silver homologues.

The influence of relativistic effects on the optimized structures can be observed in 2-M as well. If relativistic effects are not considered, the M–M bond lengthens by 0.097 Å for Au, 0.046 Å for Ag, and 0.015 Å for Cu, respectively (Table 1), which for gold is slightly smaller than that for the corresponding 1-Au compound. Furthermore, the Au–O bonds in nonrelativistic 2-Au are significantly more symmetric.

While it is obvious how dimer 1-M dissociates, for bridged 2-M compound we had to place two ligands on one metal center producing a four-coordinated monomer as shown in Figure 2

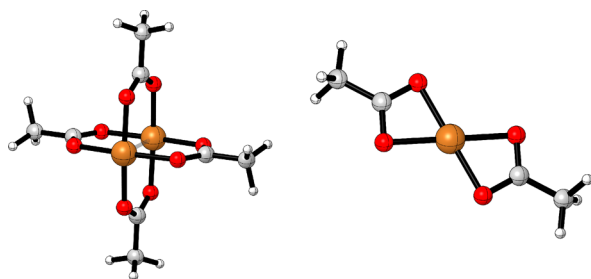


Figure 2. Optimized structures for 2-Cu (left) and its monomer (right).

for the corresponding copper compound. This makes a direct comparison with BDEs of the 1-M species difficult. Nevertheless, for the BDE, the thermodynamic stabilities calculated at the relativistic level of theory follow the trend 2-Cu > 2-Ag > 2-Au with the copper dimer being nearly twice as stable as the gold compound (Table 3). Interestingly, relativistic effects in the BDEs are relatively small compared to the 1-M compounds, i.e., the BDEs of the silver and copper dimers only change marginally whereas a somewhat larger destabilization of 21.2 kJ/mol is obtained for the gold complex (Table 3). This coincides with the appearance of more symmetrical Au–O bond lengths. This relativistic bond destabilization, which goes along with a relativistic bond contraction, sounds counter-intuitive, but it has been observed before for Au(I) diatomic

compounds with strongly electronegative ligands such as fluorine.^{19,20,35} However, in this case we need to consider the different ligand binding in the dimer, where we have bridging ligands, compared to the monomer, despite the fact that in both cases we have a four-coordinated gold atom with respect to the surrounding oxygen atoms; see Figure 2.

A simple test was performed to estimate the effect of widening the O–O distance of the acetate ligands when bonding modes to the metal atoms change from the monomer to the dimer: The O–O distance in (relativistic) 2-Cu monomer is around 0.100 Å shorter compared to that of the dimer. Optimizing the monomer in which the O–O distance is fixed to the value in the dimer increases the energy by only around 9 kJ/mol. Therefore, the steric contribution to the BDE through geometrical changes is only minor.

The BDE does not give a direct measure of the strength of the metal–metal bonding in system 2-M. A better measure comes from the bonding analysis as detailed below. The antiferromagnetic coupling can be estimated from the difference between the triplet and the singlet BS solutions. While the energy difference between the two states is small for 2-Cu (3.2 kJ/mol), this singlet–triplet gap becomes significantly larger for 2-Ag (6.9 kJ/mol) and for 2-Au (17.6 kJ/mol).

The ELF's for the 2-M compounds show, as in the case of 1-M, how much more diffuse the valence 5d-electron shell of relativistic gold atoms is compared to the nonrelativistic result and that for the other metals (Figure 3). The asymmetric Au–O interactions are visible in relativistic 2-Au and to a smaller extent in nonrelativistic 2-Au. Although there is some visible accumulation of electron density between the gold atoms indicating stronger bonding, this does not lead to a stronger M–M bond compared to the silver and copper homologues.

The Löwdin population analyses show again an increase in the 6s orbital population for the gold atom due to relativistic effects (Table 2). The atomic partial charges for 2-M reveal that the Cu and Ag atoms are significantly positively charged while Au in relativistic 2-Au is close to being neutral. Therefore, the oxygen–metal bonds in 2-Ag and 2-Cu should be considered to be more of ionic character.

A more detailed analysis of specific interatomic interactions for the weaker M–M bonding in the 2-M compounds can be obtained from QTAIM,²⁹ which uses the Laplacian of the electron density in a molecule as the basis for a topological bonding analysis. It was possible to locate bond critical points (BCP) between atoms and evaluate particular properties to characterize chemical bonding (see Table S2). An important quantity in this context is the energy density $-H$ at a BCP, which can be seen as a measure for the strength of a bonding interaction.³⁶

The energy densities for relativistic and nonrelativistic 2-Cu show that direct copper–copper interaction in the dimer is very weak, while the Cu–O bonds are symmetric and strong (Table S2). It is therefore the bridge that is holding the two copper atoms together. The metal–metal bonding interactions in 2-Ag and 2-Au are very similar and stronger than that in the copper homologue, influenced by relativistic effects. While the Ag–O bonds are predicted to be roughly equally strong (but weaker than Cu–O) and unaffected by relativistic effects, there are two groups of Au–O bonds in 2-Au when computed relativistically: a stronger one which has a higher energy density and shorter bond lengths at the BCP than the Cu–O bonds and a weaker one with 25% of that strength with longer bond lengths. In the nonrelativistic calculation, however, both Au–O bonds are

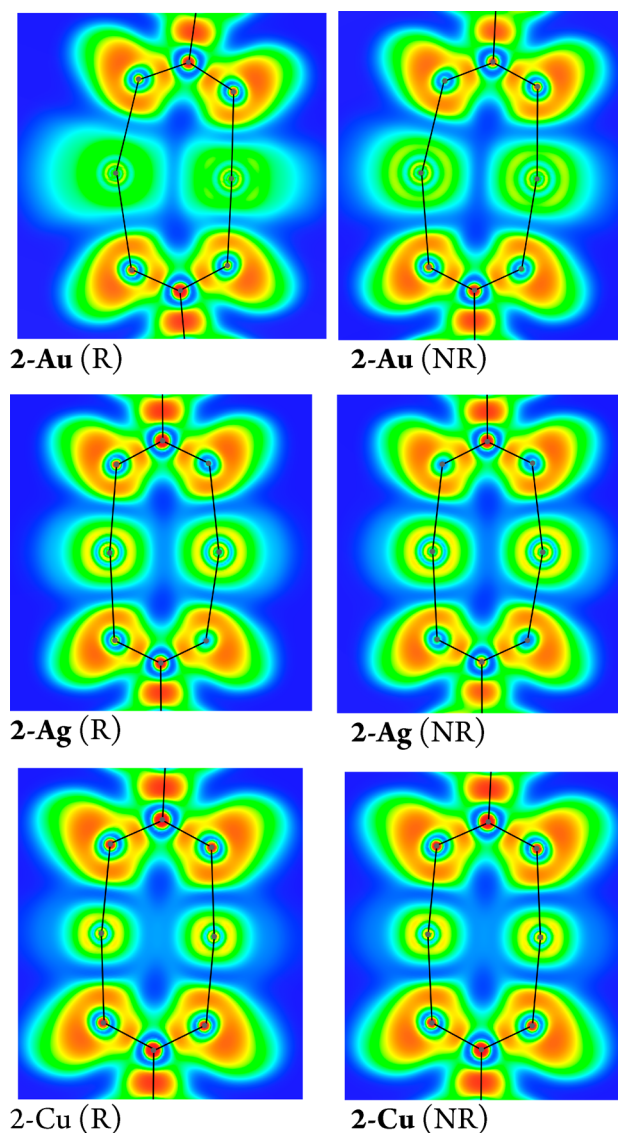


Figure 3. ELF for the M–M bonds in relativistically (R) and nonrelativistically (NR) calculated model systems 2-M.

computed to be very similar and approximately as strong as the Ag–O bonds.

In general, the bonding situation in 2-Au can be described in the following way: Each gold atom prefers to establish two strong bonds with the ligands instead of four intermediate ones like in the silver and copper dimers. This can be attributed to gold preferring a linear coordination and to its higher electronegativity, leading to more covalent bonding with the oxygen atoms. Also, the small bond dissociation energy for the gold dimer explains why this compound has not been observed yet. Here we mention that gold prefers bonding to soft ligand atoms rather than hard ones such as oxygen. Copper and silver atoms stay positively charged and engage in more ionic bonding interactions, equally distributed over the ligands. Metal–metal interactions are present, but generally very weak, and stability is provided by the bridging ligands.

CONCLUSION

We have shown how relativistic effects have an impact on the binding mode of coinage metal(II) dimers in two representative model systems. The bonding situation in 1-Au with a direct,

covalent metal–metal bond is favorable for gold as relativistic effects lead to an increased 6s orbital population, electron accumulation along the metal–metal axis, and consequently a much stronger intermetallic bond. For Ag and Cu, this bonding type is less beneficial because relativistic effects do not affect these metals as strongly, and the trend in the thermodynamic stability is therefore 1-Au > 1-Ag > 1-Cu.

For the 2-M dimers including bridging ligands with oxygen atoms, the setting is reversed: Here, it is much more preferable to engage with the ligands in four ionic bonds per metal atom. This is easy to achieve for the electropositive Cu and Ag atoms. However, relativistic effects make gold a very electronegative metal and as a consequence lead to an asymmetric bonding situation with the ligands, resulting in two strong, covalent bonds and two much weaker, ionic bonds per gold atom. Although direct metal–metal interactions are present in those complexes as well, they contribute less. We therefore find the trend 2-Cu > 2-Ag > 2-Au in the corresponding dimer stabilities. In order to achieve higher stability for such systems, softer ligands should be used to push more electron density into gold to facilitate stronger intermetallic bonding. In any case, our findings nicely agree with the experimental observation that only [Cu₂(OAc)₄·2H₂O] is known and not the corresponding gold compound.

ASSOCIATED CONTENT

Supporting Information

The Supporting Information is available free of charge on the ACS Publications website at DOI: 10.1021/acs.inorgchem.7b02434.

Bond dissociation enthalpies for compounds 1-M and 2-M, quantum theory of atoms in molecule (QTAIM) values for 2-M, and cartesian coordinates of all dimer and monomer structures obtained at the relativistic and nonrelativistic level of theory for compounds 1-M and 2-M (PDF)

AUTHOR INFORMATION

Corresponding Authors

*E-mail: paul.jerabek@gmail.com.

*E-mail: H.Schmidbaur@lrz.tu-muenchen.de.

*E-mail: p.a.schwerdtfeger@massey.ac.nz.

ORCID

Paul Jerabek: 0000-0002-2995-9755

Peter Schwerdtfeger: 0000-0003-4845-686X

Notes

The authors declare no competing financial interest.

ACKNOWLEDGMENTS

We acknowledge financial support by the Alexander von Humboldt Foundation (Bonn, Germany).

REFERENCES

- (1) (a) Laguna, A.; Laguna, M. Coordination chemistry of gold(II) complexes. *Coord. Chem. Rev.* **1999**, 193–195, 837–856. (b) Raubenheimer, H. G.; Schmidbaur, H. The late start and amazing upswing in gold chemistry. *J. Chem. Educ.* **2014**, 91, 2024–2036. (c) Mohamed, A. A.; Abdou, H. E.; Fackler, J. P., Jr. Coordination chemistry of gold(II) with amidinate, thiolate and ylide ligands. *Coord. Chem. Rev.* **2010**, 254, 1253–1259. (d) Schmidbaur, H.; Dash, K. C. Compounds of gold in unusual oxidation states. *Adv. Inorg. Chem.* **1982**, 25, 239–266. (e) Mirzadeh, N.; Bennett, M. A.; Bhargava, S. K. Cycloaurated

complexes of aryl carbanions: Digold(I), Digold(II) and beyond. *Coord. Chem. Rev.* **2013**, *257*, 2250–2273. (f) Nilakantan, L.; Pichaandi, K. R.; Abu-Omar, M. M.; McMillin, D. R.; Sharp, P. R. Synthesis, characterization and DFT study of digold(II) naphth-di-yl complex. *J. Organomet. Chem.* **2017**, *844*, 30–34. (g) Đurović, M. D.; Bugarić, Ž. D.; van Eldik, R. Stability and reactivity of gold compounds - From fundamental aspects to applications. *Coord. Chem. Rev.* **2017**, *338*, 186–206.

(2) (a) Preiß, S.; Förster, C.; Otto, S.; Bauer, M.; Müller, P.; Hinderberger, D.; Hashemi Haeri, H.; Carella, L.; Heinze, K. Structure and reactivity of a mononuclear gold(II) complex. *Nat. Chem.* **2017**, *2836*. (b) Heinze, K. The Quest for Mononuclear Gold(II) and its Potential Role in Photocatalysis and Drug Action. *Angew. Chem., Int. Ed.* **2017**, DOI: 10.1002/anie.201708349, in press.

(3) Xiong, X.-G.; Pyykkö, P. Unbridged Au(II)-Au(II) bonds are theoretically allowed. *Chem. Commun.* **2013**, *49*, 2103–5.

(4) Wickleder, M. S. AuSO₄: A True Gold(II) Sulfate with an Au₂⁴⁺ Ion. *Z. Anorg. Allg. Chem.* **2001**, *627*, 2112–2114.

(5) (a) Yam, V. W.-W.; Choi, S. W.-K.; Cheung, K.-K. Synthesis, photophysics and thermal redox reactions of a [Au(dppn)Cl]₂²⁺ dimer with an unsupported Au(II)-Au(II) bond. *Chem. Commun.* **1996**, 1173–1174. (b) Yam, V. W.-W.; Li, C.-K.; Chan, C.-L.; Cheung, K.-K. Synthesis, Structural Characterization, and Photophysics of Dinuclear Gold(II) Complexes. *Inorg. Chem.* **2001**, *40*, 7054–7058. (c) Coetzee, J.; Gabrielli, W. F.; Coetzee, K.; Schuster, O.; Nogai, S. D.; Cronje, S.; Raubenheimer, H. G. Structural studies of gold(I, II, and III) compounds with pentafluorophenyl and tetrahydrothiophene ligands. *Angew. Chem., Int. Ed.* **2007**, *46*, 2497–2500. (d) Zopes, D.; Hegemann, C.; Tyrra, W.; Mathur, S. [(CF₃)₄Au₂(C₃H₅N)₂] – a new alkyl gold(II) derivative with a very short Au–Au bond. *Chem. Commun.* **2012**, *48*, 8805–8805. (e) Roşca, D. A.; Smith, D. A.; Hughes, D. L.; Bochmann, M. A thermally stable gold(III) hydride: synthesis, reactivity, and reductive condensation as a route to gold(II) complexes. *Angew. Chem., Int. Ed.* **2012**, *51*, 10643–10646. (f) Dann, T.; Roşca, D.-A.; Wright, J. A.; Wildgoose, G. G.; Bochmann, M. Electrochemistry of Au(II) and Au(III) pincer complexes: determination of the Au(II)–Au(II) bond energy. *Chem. Commun.* **2013**, *49*, 10169–10171. (g) Yurin, S.; Lemenovskii, D.; Grandberg, K.; Il'ina, I.; Kuz'mina, L. Synthesis and structure of the first dinuclear gold complex with the Au–Au bond containing no bridging ligands. *Russ. Chem. Bull.* **2003**, *52*, 2752–2753.

(6) Grochala, W.; Majej, Z. Chemistry of silver(II): a cornucopia of peculiarities. *Philos. Trans. R. Soc., A* **2015**, *373*, 20140179–20140179.

(7) Malinowski, P. J.; Derzsi, M.; Majej, Z.; Jagličić, Z.; Gawel, B.; Łasocha, W.; Grochala, W. Ag(II)SO₄: a genuine sulfate of divalent silver with anomalously strong one-dimensional antiferromagnetic interactions. *Angew. Chem., Int. Ed.* **2010**, *49*, 1683–1686.

(8) Walker, N. R.; Wright, R. R.; Stace, A. J. Stable Ag(II) coordination complexes in the gas phase. *J. Am. Chem. Soc.* **1999**, *121*, 4837–4844.

(9) Melník, M.; Kabešová, M.; Dunaj-Jurčo, M.; Holloway, C. E. Copper(II) Coordination Compounds: Classification and Analysis of Crystallographic and Structural Data. *J. Coord. Chem.* **1997**, *41*, 35–182.

(10) Greenwood, N. N.; Earnshaw, A. In *Chemistry of the Elements*; Pergamon: Oxford, 1984; p 1380 ff.

(11) (a) Schmidbaur, H.; Mandl, J. R.; Wagner, F. E.; Van de Vondel, D. F.; Van der Kelen, G. P. ESCA and Mössbauer study of compounds of gold in the oxidation states + I, + II, and + III. *J. Chem. Soc., Chem. Commun.* **1976**, 170–172. (b) Schmidbaur, H.; Hartmann, C.; Wagner, F. E. The Recoil-Free Fraction of the γ -Resonance in ¹⁹⁷Au Mössbauer Spectroscopy; Findings from Measurements of Polynuclear, Mixed-Valent Ylide Complexes. *Angew. Chem., Int. Ed. Engl.* **1987**, *26*, 1148–1150.

(12) van Niekerk, J. N.; Schoening, F. R. L. A new type of copper complex as found in the crystal structure of cupric acetate, Cu₂(CH₃COO)₄ • 2 H₂O. *Acta Crystallogr.* **1953**, *6*, 227–232.

(13) (a) Shee, N. K.; Verma, R.; Kumar, D.; Datta, D. On copper-copper bond in hydrated cupric acetate. *Comput. Theor. Chem.* **2015**,

1061, 1–5. (b) Brown, G. M.; Chidambaram, R. Dinuclear copper(II) acetate monohydrate: a redetermination of the structure by neutron-diffraction analysis. *Acta Crystallogr., Sect. B: Struct. Crystallogr. Cryst. Chem.* **1973**, *29*, 2393–2403. (c) Bertolotti, F.; Forni, A.; Gervasio, G.; Marabello, D.; Diana, E. Experimental and theoretical charge density of hydrated cupric acetate. *Polyhedron* **2012**, *42*, 118–127.

(14) Hay, P. J.; Thibeault, J. C.; Hoffmann, R. Orbital interactions in metal dimer complexes. *J. Am. Chem. Soc.* **1975**, *97*, 4884–4899.

(15) Porter, L. C.; Fackler, J. P., Jr. Structure of the first example of an organometallic dinuclear gold(II) complex possessing bonds to oxygen. *Acta Crystallogr., Sect. C: Cryst. Struct. Commun.* **1986**, *42*, 1128–1131.

(16) Hermann, A.; Derzsi, M.; Grochala, W.; Hoffmann, R. AuO: Evolving from Dis- to Comproportionation and Back Again. *Inorg. Chem.* **2016**, *55*, 1278–1286.

(17) Åsbrink, S.; Norrby, L.-J. A refinement of the crystal structure of copper(II) oxide with a discussion of some exceptional E.s.d.'s. *Acta Crystallogr., Sect. B: Struct. Crystallogr. Cryst. Chem.* **1970**, *26*, 8–15.

(18) (a) Scatturin, V.; Bellon, P. L.; Salkind, A. J. The structure of silver oxide determined by means of neutron diffraction. *J. Electrochem. Soc.* **1961**, *108*, 819–822. (b) Allen, J. P.; Scanlon, D. O.; Watson, G. W. Electronic structure of mixed-valence silver oxide AgO from hybrid density-functional theory. *Phys. Rev. B: Condens. Matter Mater. Phys.* **2010**, *81*, 161103.

(19) (a) Pyykkö, P. Relativistic effects in structural chemistry. *Chem. Rev.* **1988**, *88*, 563–594. (b) Kaltsoyannis, N. Relativistic effects in inorganic and organometallic chemistry. *J. Chem. Soc., Dalton Trans.* **1997**, 1–12. (c) Pyykkö, P. Theoretical chemistry of gold. *Angew. Chem., Int. Ed.* **2004**, *43*, 4412–4456. (d) Iliaš, M.; Kellö, V.; Urban, M. Relativistic effects in atomic and molecular properties. *Acta Phys. Slovaca* **2010**, *60*, 259–391. (e) Pyykkö, P. Relativistic effects in chemistry: more common than you thought. *Annu. Rev. Phys. Chem.* **2012**, *63*, 45–64.

(20) (a) Schwerdtfeger, P.; Dolg, M.; Schwarz, W. H. E.; Bowmaker, G. A.; Boyd, P. D. W. Relativistic effects in gold chemistry. I. Diatomic gold compounds. *J. Chem. Phys.* **1989**, *91*, 1762–1774. (b) Schwerdtfeger, P. Relativistic effects in gold chemistry. 2. The stability of complex halides of gold(III). *J. Am. Chem. Soc.* **1989**, *111*, 7261–7262. (c) Schwerdtfeger, P.; Boyd, P. D. W.; Burrell, A. K.; Robinson, W. T.; Taylor, M. J. Relativistic effects in gold chemistry. 3. Gold(I) complexes. *Inorg. Chem.* **1990**, *29*, 3593–3607. (d) Schwerdtfeger, P. Relativistic and electron-correlation contributions in atomic and molecular properties: benchmark calculations on Au and Au₂. *Chem. Phys. Lett.* **1991**, *183*, 457–463. (e) Schwerdtfeger, P.; Boyd, P. D. W.; Brienne, S.; Burrell, A. K. Relativistic effects in gold chemistry. 4. Gold(III) and gold(V) compounds. *Inorg. Chem.* **1992**, *31*, 3411–3422. (f) Theilacker, K.; Schlegel, H. B.; Kaupp, M.; Schwerdtfeger, P. Relativistic and Solvation Effects on the Stability of Gold(III) Halides in Aqueous Solution. *Inorg. Chem.* **2015**, *54*, 9869–9875.

(21) (a) Schwerdtfeger, P. Relativistic effects in properties of gold. *Heteroat. Chem.* **2002**, *13*, 578–584. (b) Schwerdtfeger, P.; Lein, M. In *Gold Chemistry. Current Trends and Future Directions*; Mohr, F., Ed.; Wiley-VCH: Weinheim, 2009; pp 183–247.

(22) (a) Baerends, E.-J.; Schwarz, W. E.; Schwerdtfeger, P.; Snijders, J. G. Relativistic atomic orbital contractions and expansions: magnitudes and explanations. *J. Phys. B: At., Mol. Opt. Phys.* **1990**, *23*, 3225–3240. (b) Autschbach, J.; Siekierski, S.; Seth, M.; Schwerdtfeger, P.; Schwarz, W. Dependence of relativistic effects on electronic configuration in the neutral atoms of d- and f-block elements. *J. Comput. Chem.* **2002**, *23*, 804–813.

(23) (a) Pyykkö, P. Strong closed-shell interactions in inorganic chemistry. *Chem. Rev.* **1997**, *97*, 597–636. (b) Pyykkö, P.; Runeberg, N.; Mendizabal, F. Theory of the d¹⁰–d¹⁰ Closed-Shell Attraction: I. Dimers Near Equilibrium. *Chem. - Eur. J.* **1997**, *3*, 1451–1457. (c) Hermann, H. L.; Boche, G.; Schwerdtfeger, P. Metallophilic Interactions in Closed-Shell Copper(I) Compounds – A Theoretical Study. *Chem. - Eur. J.* **2001**, *7*, 5333–5342. (d) Wang, S.-G.; Schwarz, W. E. Quasi-relativistic density functional study of aurophilic interactions. *J. Am. Chem. Soc.* **2004**, *126*, 1266–1276. (e) O'Grady,

E.; Kaltsoyannis, N. Does metallophilicity increase or decrease down group 11? Computational investigations of $[\text{Cl}-\text{M}-\text{PH}_3]_2$ ($\text{M} = \text{Cu}, \text{Ag}, \text{Au}, [\text{111}]$). *Phys. Chem. Chem. Phys.* **2004**, *6*, 680–687. (f) Assadollahzadeh, B.; Schwerdtfeger, P. A comparison of metallophilic interactions in group 11 $[\text{X}-\text{M}-\text{PH}_3]_n$ ($n = 2-3$) complex halides ($\text{M} = \text{Cu}, \text{Ag}, \text{Au}; \text{X} = \text{Cl}, \text{Br}, \text{I}$) from density functional theory. *Chem. Phys. Lett.* **2008**, *462*, 222–228. (g) Schmidbaur, H.; Schier, A. Auophilic interactions as a subject of current research: an update. *Chem. Soc. Rev.* **2012**, *41*, 370–412. (h) Schmidbaur, H.; Schier, A. Argentophilic interactions. *Angew. Chem., Int. Ed.* **2015**, *54*, 746–784.

(24) (a) Jiang, Y.; Alvarez, S.; Hoffmann, R. Binuclear and polymeric gold(I) complexes. *Inorg. Chem.* **1985**, *24*, 749–757. (b) Pyykkö, P.; Mendizabal, F. Theory of $d^{10}-d^{10}$ Closed-Shell Attraction. III. Rings. *Inorg. Chem.* **1998**, *37*, 3018–3025.

(25) (a) Grimme, S.; Antony, J.; Ehrlich, S.; Krieg, H. A Consistent and Accurate Ab Initio Parametrization of Density Functional Dispersion Correction (DFT-D) for the 94 Elements H-Pu. *J. Chem. Phys.* **2010**, *132*, 154104–154104. (b) Grimme, S.; Ehrlich, S.; Goerigk, L. Effect of the Damping Function in Dispersion Corrected Density Functional Theory. *J. Comput. Chem.* **2011**, *32*, 1456–1465.

(26) (a) Neese, F. The ORCA program system. *Wiley Interdisciplinary Reviews: Computational Molecular Science* **2012**, *2*, 73–78. (b) Schäfer, A.; Horn, H.; Ahlrichs, R. Fully Optimized Contracted Gaussian-Basis Sets for Atoms Li to Kr. *J. Chem. Phys.* **1992**, *97*, 2571–2577. (c) Weigend, F.; Ahlrichs, R. Balanced basis sets of split valence, triple zeta valence and quadruple zeta valence quality for H to Rn: Design and assessment of accuracy. *Phys. Chem. Chem. Phys.* **2005**, *7*, 3297–305. (d) Stephens, P. J.; Devlin, F. J.; Chabalowski, C. F.; Frisch, M. J. Ab Initio Calculation of Vibrational Absorption and Circular Dichroism Spectra Using Density Functional Force Fields. *J. Phys. Chem.* **1994**, *98*, 11623–11627. (e) Becke, A. D. Density-functional thermochemistry. III. The role of exact exchange. *J. Chem. Phys.* **1993**, *98*, 5648–5652. (f) Lee, C.; Yang, W.; Parr, R. G. Development of the Colle-Salvetti correlation-energy formula into a functional of the electron density. *Phys. Rev. B: Condens. Matter Mater. Phys.* **1988**, *37*, 785–789. (g) Vosko, S. H.; Wilk, L.; Nusair, M. Accurate spin-dependent electron liquid correlation energies for local spin density calculations: a critical analysis. *Can. J. Phys.* **1980**, *58*, 1200–1211.

(27) Neese, F.; Wennmohs, F.; Hansen, A.; Becker, U. Efficient, approximate and parallel Hartree-Fock and hybrid DFT calculations. A 'chain-of-spheres' algorithm for the Hartree-Fock exchange. *Chem. Phys.* **2009**, *356*, 98–109.

(28) (a) Andrae, D. Diploma Thesis. 1989. (b) Dolg, M.; Wedig, U.; Stoll, H.; Preuss, H. Energy-adjusted ab-initio pseudopotentials for the first row transition elements. *J. Chem. Phys.* **1987**, *86*, 866–872. (c) Figgen, D.; Rauhut, G.; Dolg, M.; Stoll, H. Energy-consistent pseudopotentials for group 11 and 12 atoms: adjustment to multi-configuration Dirac-Hartree-Fock data. *Chem. Phys.* **2005**, *311*, 227–244.

(29) Bader, R. F. W. *Atoms in Molecules: A Quantum Theory*. University Press: Oxford, 1994.

(30) Lu, T.; Chen, F. Multiwfn: A multifunctional wavefunction analyzer. *J. Comput. Chem.* **2012**, *33*, 580–592.

(31) Löwdin, P.-O. On the Non-Orthogonality Problem Connected with the Use of Atomic Wave Functions in the Theory of Molecules and Crystals. *J. Chem. Phys.* **1950**, *18*, 365–275.

(32) (a) Pantazis, D. A.; Chen, X. Y.; Landis, C. R.; Neese, F. All-electron scalar relativistic basis sets for third-row transition metal atoms. *J. Chem. Theory Comput.* **2008**, *4*, 908–919. (b) Van Wüllen, C. Molecular density functional calculations in the regular relativistic approximation: Method, application to coinage metal diatomics, hydrides, fluorides and chlorides, and comparison with first-order relativistic calculations. *J. Chem. Phys.* **1998**, *109*, 392–399.

(33) (a) Becke, A. D.; Edgecombe, K. E. A simple measure of electron localization in atomic and molecular systems. *J. Chem. Phys.* **1990**, *92*, 5397–5403. (b) Savin, A.; Nesper, R.; Wengert, S.; Fässler, T. F. ELF: The Electron Localization Function. *Angew. Chem., Int. Ed. Engl.* **1997**, *36*, 1808–1832.

(34) (a) Noodleman, L. Valence bond description of antiferromagnetic coupling in transition metal dimers. *J. Chem. Phys.* **1981**, *74*, 5737–5743. (b) Noodleman, L.; Case, D. A. Density-Functional Theory of Spin Polarization and Spin Coupling in Iron-Sulfur Clusters. *Adv. Inorg. Chem.* **1992**, *38*, 423–470. (c) Ruiz, E.; Cano, J.; Alvarez, S.; Alemany, P. Magnetic coupling in end-on azido-bridged transition metal complexes: A density functional study. *J. Am. Chem. Soc.* **1998**, *120*, 11122–11129. (d) Onofrio, N.; Mouesca, J. M. Valence bond/broken symmetry analysis of the exchange coupling constant in copper(II) dimers. Ferromagnetic contribution exalted through combined ligand topology and (singlet) covalent-ionic mixing. *J. Phys. Chem. A* **2010**, *114*, 6149–6156.

(35) Schwerdtfeger, P.; McFeaters, J. S.; Liddell, M. J.; Hrušák, J.; Schwarz, H. Spectroscopic properties for the ground states of AuF, AuF⁺, AuF₂, and Au₂F₂: A pseudopotential scalar relativistic Møller–Plesset and coupled-cluster study. *J. Chem. Phys.* **1995**, *103*, 245–252.

(36) Cremer, D.; Kraka, E. Chemical Bonds without Bonding Electron Density? Does the Difference Electron-Density Analysis Suffice for a Description of the Chemical Bond? *Angew. Chem., Int. Ed. Engl.* **1984**, *23*, 627–628.